Role of Surface Geometric Patterns and Parameters in the Dispersion Relations of Spoof Surface Plasmon Polaritons at Microwave Frequency

Rana Sadaf Anwar, Lingfeng Mao, and Huansheng Ning*

School of Computer and Communication Engineering
University of Science and Technology Beijing, Beijing, 100083, China
engr_rs@126.com, lingfengmao@ustb.edu.cn, *ninghuansheng@ustb.edu.cn

Abstract ─ Spoof surface plasmon polaritons (SSPPs) can be excited using geometric shapes on conducting surfaces in microwave (MW) regime. They are eminent as compared to the conventional microstrip (MS) transmission lines, due to their better efficiency and compactness in high density and high-speed circuitry. In this work, we compare normalized dispersion curves (DCs) of different groove shapes engineered on the planar metallic strip with the variation of geometric parameters of the structure, which are obtained by Eigen-mode solver of ANSYS's HFSS. It is found the dispersion characteristics are determined by the shape and the asymptotic frequency can finely be tuned through the geometric parameters. All DCs deviate further from the light line indicating slow propagation of SSPPS. The performance of rectangular grooves is clearly outstanding; however, the circular grooves behave comparably better than Vee-groove. Further, a low pass plasmonic filter has been proposed with semi-circular gradient subwavelength grooves designed on a planar metallic strip with transition sections to match both the impedance and momentum of MS line and the plasmonic waveguide. Results of S-parameters and magnitude of electric field distributions show excellent transmission efficiency from fast guided wave to slow SSPPs. It is also observed that the confinement of such surface waves is dependent on the geometric parameters which can be useful in plasmonic structure engineering and fine-tuning the cutoff frequencies, hence posing a new prospect for advanced plasmonic integrated devices and circuits.

Index Terms ─ Microwave, plasmonics, surface plasmon polaritons, sub-wavelength, surface geometry.

I. INTRODUCTION

Manipulating the electromagnetic waves through subwavelength apertures has invoked the interest of many researchers and formed the basis of extensive investigation in the field of plasmonics, after the discovery of extraordinary transmission through nanohole arrays in the metallic film by Ebbesen et al. [1]. Applications of plasmonics are focused in diverse fields such as Surface-Enhanced Raman Scattering [2], surface plasmon resonance sensors [3], and surface plasmon spectroscopy systems [4]. Numerous areas have been flourished by plasmonics, ranging from chemistry, biology, physics, and material science [5-7].

Surface plasmon polaritons **(**SPPs) are the self-sustaining and propagating electromagnetic (EM) waves, which are provoked on the metal-dielectric interface in the optical regime where the incident energy is highly accumulated across the edges of the periodic corrugations in metal film and so it can easily cross through [1, 8]. SPPs have much smaller wavelength as compared to the light of incidence. Once SPPs are excited, they travel in a direction parallel to the metal-dielectric interface. They are evanescent by nature, and so they decay exponentially along the perpendicular direction of the metal-dielectric interface. The propagation of SPPs can be manipulated through couplers and waveguides. However, there is a mismatch in momentum between SPPs and free space photon of light, due to bound nature of SPPs, which is evident by k-vector differences on dispersion diagrams. This mismatch depends on the surface nature of the structure. Momentum matching can be achieved by scattering of EM waves through the use of methods such as using high index prism, evanescent field coupling and grating coupling [9, 10].

Free carriers have a major contribution to the dielectric function which is of significant importance in metals and semiconductors. A classical conductivity model based on standard equations for electron motion in an electric field is referred to as the Drude model and presents the straightforward theory for the optical parameters. The dielectric constant of conducting metal film is related to plasma frequency and is given by Drude's model as:

$$\varepsilon_M(\omega) = 1 - \frac{\omega_P^2}{\omega^2 - i\Gamma\omega}, \tag{1}$$

$$\omega_P = \sqrt{ne^2 / m\varepsilon_0}. \tag{2}$$

Here, ω_P defines the plasma frequency of the metal, ω is the angular frequency of the incident electromagnetic wave, ε_0 is the permittivity of free space, Γ is the

Submitted On: June 29, 2018
Accepted On: December 25, 2018

scattering rate of electron motion, while n is the free carrier density, e and m are the charge and the mass of an electron, respectively. Usually, metals have a higher density of free electrons; therefore, their ω_P is higher. The dispersion relation for light in a metal bounded to a dielectric layer is derived by solving Maxwell's equations by substituting dielectric constant relation (1):

$$k_x = k_0 \sqrt{\frac{\varepsilon_I \varepsilon_M}{(\varepsilon_I + \varepsilon_M)}}, \quad (3)$$

The in-plane wavevector k_x, named as the momentum of SPPs (also represented by β), is a function of angular frequency [10] and is the wavevector in the plane of the un-textured surface along which it propagates. k_0 is the free-space wavevector. $\mathcal{E}_I$ and $\mathcal{E}_M$ are the frequency dependent complex dielectric functions (relative permittivity) of adjacent dielectric film and metal, respectively. It has been noticed at $\omega<\omega_P$, the condition $k_x>k_0$ is satisfied. Therefore, SPP's field decays exponentially with the distance from the surface, along with the perpendicular direction of the metal-dielectric interface. The occurrence of this field is temporary by nature, and so it is limited to the surface of the metal. The field confinement of SPPs is tighter for higher values of wavevector.

In contrast to the optical regime, the metal behaves as a perfect electric conductor (PEC) at lower frequencies. To overcome this problem, properties similar to the SPPs have been achieved by using plasmonic metamaterials proposed by many researchers by use of subwavelength textured structures after the proposal by Pendry et al. [11]. Different shapes of metallic subwavelength aperture arrays, grooves or single slit structures are being explored, working at the microwave to terahertz regime. Such textured surfaces support the propagation of surfaces waves also called as spoof SPPs (SSPPs) [12]. A lower working frequency of SPPs to gigahertz can be achieved through surface decorations, such as holes [13], metallic apertures [14, 15], rectangular gratings [16, 17], triangular corrugations [18], T-grooves [19] and elliptical grooves [20]. A review of recent progress on exciting SPPs in microwave (MW) and terahertz (THz) regimes by incorporating various subwavelength corrugated shapes on conductive or metal surfaces has been presented in [21].

It has been known that propagating EM waves on the surface of a structure have a propagation constant given as $\gamma=\alpha+j\beta$, where α represents the attenuation constant and β is the phase constant. It is known that the confinement of SSPPs mainly depends on the β (wavenumber along the direction of propagation k_x) which is related to k_0 by a related parameter of the decay constant (along tangential direction) and is given by [22]:

$$\alpha_t = \sqrt{k_x^2 - k_0^2}, \quad (4)$$

Here, $k_0=2\pi/\lambda$. It can be observed from (4) that the level of field confinement is positively related to the wavenumber in the direction of propagation.

The analysis presented in this paper gives a comparison of the dispersion curves by engineering different type of surface textures as the phenomenon of exciting SSPPs has been proved in earlier investigations on the planar conducting layer with surface decorations. We consider three geometric structure shapes to excite the SSPPs and analyze their effects on DCs (ω–β relations) in detail by performing comparisons of their dispersion and confinement capacities. It is proved that basic unit cell geometry can play a prominent role in SSPPs excitation. For example, we find that they are highly bound to the surface with rectangular corrugations and have a lower asymptotic frequency as compared to surfaces with circular/V-groove patterns. Due to the lower value of momentum mismatch for circular and V-groove structures, they are closer to the wave vector of free space (k_0). Therefore, surface texture engineering can cause prominent influence in applications of planar plasmonic metamaterials and nanophotonics.

II. DISPERSION RELATIONS AND ANALYSIS

We investigate the dispersion characteristics of SSPPs for planar metallic structures having different etched geometries by the Eigen mode solver of the commercial software package, ANSYS's High Frequency Structure Simulator (HFSS) which uses Finite element method (FEM). The TM-polarized waves are propagating in the x-direction which is along the corrugated metal plate structures as depicted in Fig. 1. The properties of SSPPs modes are primarily controlled by the geometric parameters of the structure. To perform a comparison; the structure is composed of a thin metallic strip (parameter 't' for thickness) on top of a dielectric substrate with a thickness of 2.65mm, the relative dielectric constant of 2.2 and loss tangent of 0.0009. We denote the width and depth of grooves by 'w' and 'h' respectively while the period of the structure is 'P' and height of the metallic strip is 'H' for all grooved structures as shown in Fig. 1. Firstly, to study the dispersion behavior, we start with circular groove and vary the height 'h' from 5mm to 7.5mm while 'P', 'w' and 'H' are kept constant at 20mm, 7.5mm, and 8mm respectively. The dispersion curves so obtained for the fundamental propagating mode are plotted in Fig. 2. The continuous black curve is the light line (LL), and the black dashed curve shows the DC of microstrip (un-textured) structure.

It is clear from Fig. 2 that all the dispersion curves deviate from the light line and reach a constant asymptotic frequency at the edge of the Brillouin zone which is the region in k-space which can be occupied by low "*k*" electrons without being affected by diffraction phenomenon. The DCs for SSPPs show that the asymptotic frequency is dominantly related to the depth of the grooves. As the depth of the grooves increases, the asymptotic frequency gets lower (higher β), which

implies the stronger confinement of surface waves in the circular groove strip. As the depth of grooves is decreased, the in-plane wave vector gradually approaches k_0. Therefore, the SSPPs are strongly bounded for higher in-plane wavevector and vice versa. At low frequency limit, the SSPPs dispersion curves are closer to the light line. The metal acts as a perfect electric conductor (PEC) in this regime (comprises of microwave frequency region). The dispersion relation for this limit is reduced to $k_x=k_0$ and corresponds to EM wave propagating parallel to the interface in a dielectric layer. That is the reason, at low frequency, the SSPPs behave like light.

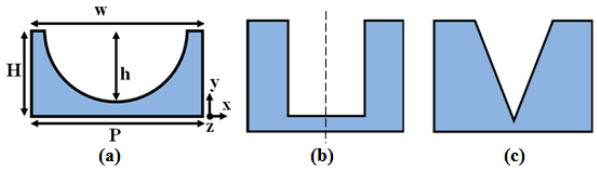

Fig. 1. Unit cell of a SSPPs structure with geometric parameters characterizing the groove geometry for: (a) Circular (Cir) groove, (b) Rectangular (Rec) groove, and (c) V (Vee) groove.

At high frequency range, as it approaches surface plasmon frequency, the propagation constant of SSPPs is greater than that of vacuum, which implies that they are more strongly confined. For example, in Fig. 2, when h=5mm, the asymptotic frequency reaches 4.3GHz, the dispersion approaches SSPP modes which propagate more gradually and localize more tightly on the surface of the semi-circular grooved metal plate.

To make a comparison among SSPPs structures with differently patterned grooves, we consider the unit cells as shown in Figs. 1 (a-c), to perform simulations. All the grooved patterns have the same geometric parametric values as for Fig. 2 along with h=7.5mm, and the dispersion relations are shown in Fig. 3. It is prominent that geometric shape and their parameters play a major role in determining the dispersion properties. All the dispersion curves deviate from the light line and increasingly become steady until they reach their asymptotic frequencies. Although all of them pose a similar trend, these curves exhibit different frequency band behavior for different grooves patterns. Noticeably, the asymptotic frequency of the rectangular groove structure is lower than other types, confirming that it has strongest field confinement of SSPPs on the surface. Circular groove dispersion behavior is better than Vee groove as it has a comparatively lower asymptotic frequency.

Single sided rectangular grooves structure on a dielectric substrate can be assumed as similar to an array of coplanar strip aligned vertically, and the dispersion relation of such a corrugated MS can be found by (5) as given in [23] where k_0 is replaced by $\sqrt{\varepsilon_{eff}}k_0$ to estimate the asymptotic frequency:

$$\sqrt{k_x^2-\varepsilon_{eff}k_0^2}=\sqrt{\varepsilon_{eff}}k_0\left(\frac{w}{P}\right)\tan\left(\sqrt{\varepsilon_{eff}}k_0h\right), \quad (5)$$

ε_{eff} is the effective permittivity where the SSPPs propagate and can be estimated by (6):

$$\varepsilon_{eff}=1+\left(\frac{\varepsilon_I-1}{2}\right)\frac{K(k')K(k_1)}{K(k)K(k_1')}, \quad (6)$$

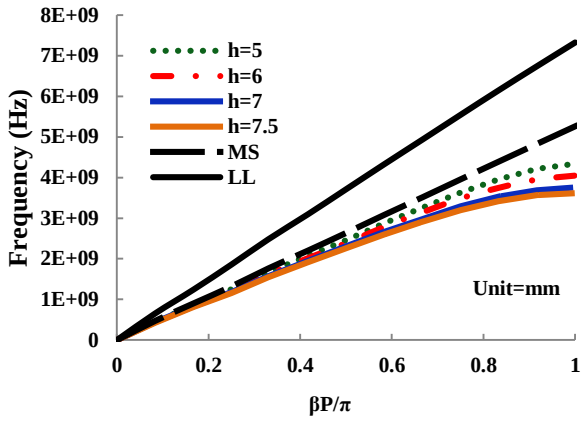

Fig. 2. Dispersion relations of SSPPs for the fundamental mode with varying circular groove depths.

Here, K represents the whole elliptic integral of the first type, $k=w/P$, $k'=\sqrt{1-k^2}$, $k_1'=\sqrt{1-k_1^2}$, and $k_1=\dfrac{\sinh\left(\pi w/4t\right)}{\sinh\left(\pi P/4t\right)}$.

Explicit effect of structure parameters on the dispersion characteristics can be understood through an analysis, by changing the parametric values. The corrugation size significantly impacts on the SSPPs characteristics. Higher is the value of groove width 'w' and height 'h', lower is the asymptotic frequency and therefore stronger is the field confinement [24].

Figure 4 depicts the effect of groove width 'w' on the dispersion curves of different SSPPs structures. Width 'w' of all three types of structures is reduced to 1mm comparatively as used in the previous analysis (7.5mm) shown in Fig. 3. A comparison of DCs for circular and rectangular grooved structures respectively is given in Fig. 5, in which groove width is reduced from 7.5mm to 1mm. It is seen that the asymptotic frequency depends prominently on the groove width and decreases when 'w' increases, indicating that this geometric parameter notably affects the confinement ability of the surface waves.

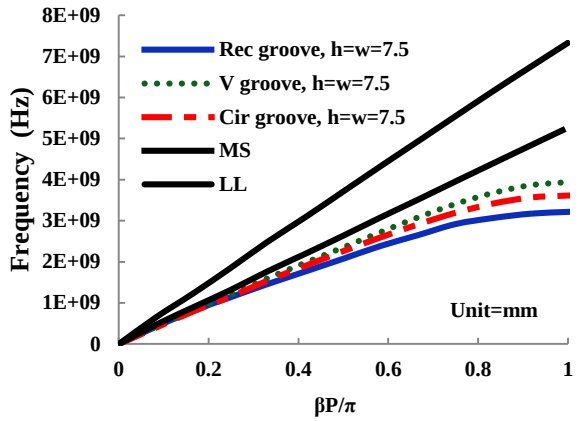

Fig. 3. Dispersion relations of SSPPs for the fundamental mode of different structures at w=h.

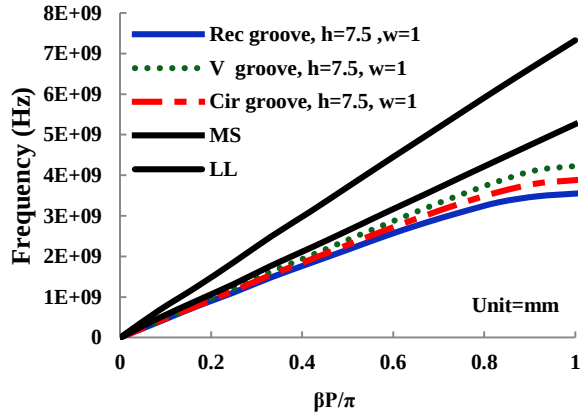

Fig. 4. Dispersion relations of SSPPs for the fundamental mode of different structures with w<<h.

Similarly, the structure size parameters, height 'H' and period 'P' of the unit cell have a prominent influence on the frequency range, but the trend of the dispersion curves remains less effective. The frequency domain is reduced with the bigger size of the structure. To estimate the impact of period 'P' on structure performance, we evaluate the dispersion relations of a unit cell having a circular groove with different 'P' values as shown in Fig. 6. The period is varied from 16mm to 24mm with a step size of 4mm with remaining parameters set equal as in Fig. 3. It is illustrated that the DCs are very sensitive to the change in period 'P' for the complete frequency range, and it is prominent that the asymptotic frequency decreases remarkably as 'P' increases. Furthermore, at a constant frequency in the SSPPs mode, the propagation constant increases as the period is increased, for example, in Fig. 6, it is demonstrated that at the asymptotic frequency of 2 GHz, $\beta 3 > \beta 2 > \beta 1$. Therefore, the length of the period can improve the field confinement ability of the grooved structures.

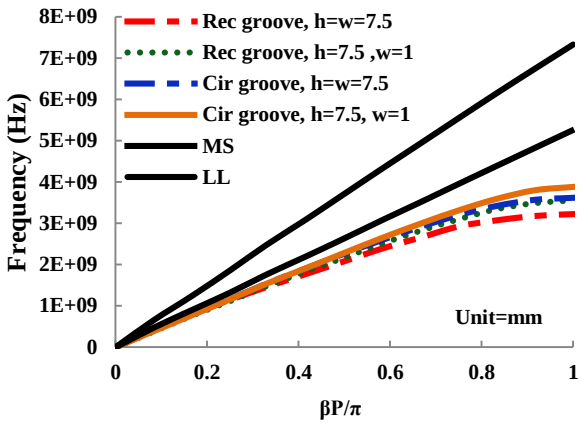

Fig. 5. Dispersion relations of SSPPs for the fundamental mode of rectangular and circular groove structure with varying groove width.

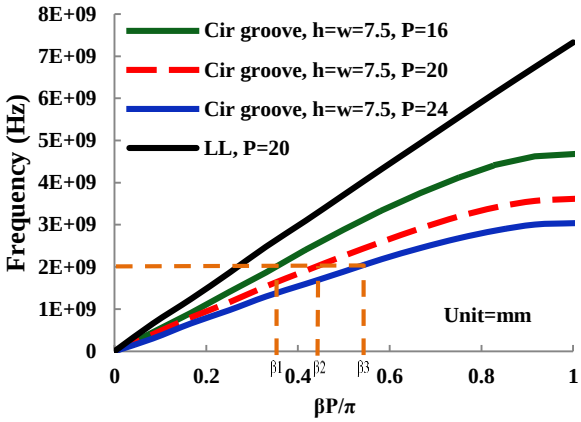

Fig. 6. Dispersion curves of SSPPs for the fundamental mode of the circular grooved with varying period length.

A. Field confinement analysis

To get a direct insight of the modal characteristics of the SSPPs on different groove structures, the magnitude electric field distributions are plotted at the cross section of unit cells (location shown by dotted line in Fig. 1 (b) and field confinement capacities are compared in Figs. 7 (a-c). The parameters are set equal as for dispersion analysis in Fig. 3. It has been clearly observed that the rectangular groove has the strongest confinement of SSPPs whereas the V-groove exhibits the weakest localization of field, therefore explicitly confirming the findings in dispersion curves of Fig. 3.

Furthermore, Figs. 8 (a-c) gives a demonstration of magnitude electric field distributions with varying groove depth, width and period for the circular groove. When the groove depth is kept constant as in the previous analysis of Fig. 7 (b) while the width is reduced to 1mm, relatively the field is not confined anymore as shown in Fig. 8 (a) and spreads into the substrate. The same effect is ratified

in the dispersion relation of Fig. 5 by a rise in asymptotic frequency.

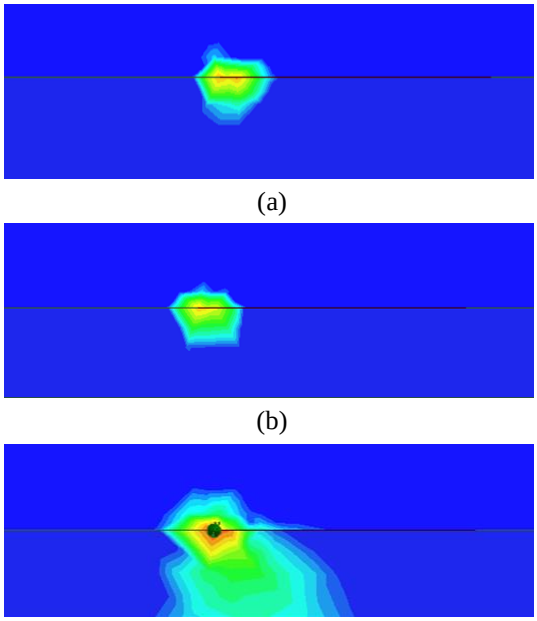

Fig. 7. Simulated magnitude electric field distribution at the cross section of the structure with h=w=7.5: (a) Rectangular groove, (b) Circular grooven, and (c) Vee groove.

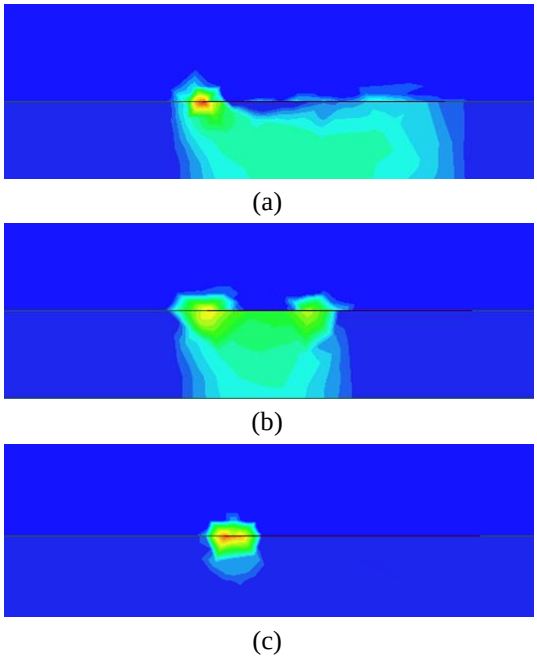

Fig. 8. Simulated magnitude electric field distribution at the cross section of the structure: (a) Circular groove with h=7.5, w=1mm, (b) Circular groove with h=w=5, and (c) Circular groove with h=w=7.5 and P=24mm.

Therefore, to maintain the frequency back to the lower value, the only solution is to increase the groove's height; however, it will cause the structure dimensions to augment [25]. Figure 8 (b) depicts the delocalization of electric field when both the depth and width of groove is decreased to 5mm. However, in contrast, when the period is raised to 24mm with the maximum groove depth of 7.5mm, an enhanced field confinement ability is observed, fortifying the results in Fig. 6 by a reduction in asymptotic frequency.

As demonstrated previously, the ability to confine surface waves is highly responsive to the period length of the structure as well as to the corrugation depth and width. When the frequency of the incident wave reaches near the asymptotic frequency, it couples deeper into the grooves, and so electromagnetic field is confined on the surface because of the higher mismatch of wavevector between SSPPs and free space photon of light. While, at a lower frequency, propagation of EM waves exhibits weaker confinement on the surface, consequently the dispersion characteristics are close to the light line. Hence, the design of subwavelength SSPPs structures in microwave regime is facilitated by controlling the asymptotic frequency with the variation of groove shape, its depth, width and period length on the surface of the structure.

III. STRUCTURE DESIGN OF LOW-PASS PLASMONIC FILTER

From dispersion relations, it has been noticed that the wavevector of SSPPs are highly mismatched to that of light line especially when the asymptotic frequency is reached. This will result in extremely less transmission performance. Therefore, to efficiently feed in and extract out the maximum power, a plasmonic filter with transition structure is designed. In contrast to planar defected MS filter proposed in [26-28] and earlier investigated plasmonic filters based on rectangular gratings [17], triangular corrugations [18], and T-grooves [19], here we investigate SSPPs based on semi-circular gratings etched on planar metallic strip which is highly unexplored textured surface until now to the best of our knowledge. It consists of a microstrip line with gradient subwavelength semi-circular grooves with depth h varying from 7mm to 3mm with a step of 1mm designed on a dielectric substrate as investigated in Section II as shown in Fig. 9. Two transition links at both ends provide a gradient momentum and impedance matching; therefore, conversion of guided waves to spoof SPPs is achieved. The dimensions are given here: L_1=2.5mm, L_2=60mm, L_3=105mm, H=7.5mm, P=15mm. A is the traditional microstrip section, B is the mode transition section and C is the SSPPs section with h=7mm and w=14mm. To evaluate the performance of this filter structure, the S-parameters are obtained by simulation software ANSYS's HFSS and shown in Fig. 10. The cutoff frequency (f_c) of the filter is 4.91GHz which is mainly anticipated by the asymptotic frequency of SSPPs mode support by the

waveguide region C. An efficient passband is achieved with S11 less than -10dB from 0.45 to 4.91GHz. The upper stopband covers a frequency range from 5.11 to 10GHz with rejection less than -18dB (even < -25dB from 5.15 to 8.11GHz) which points to an outstanding realization of impedance matching between the MS and the SSPPs.

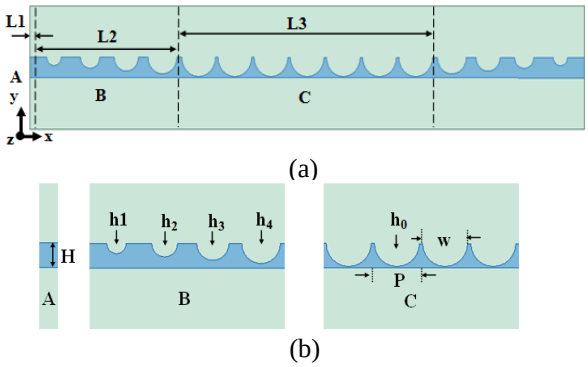

Fig. 9. (a) The configuration of the proposed plasmonic filter showing the top view of SSPPs structure with three sections. (b) Detailed view of Region A, B, and C.

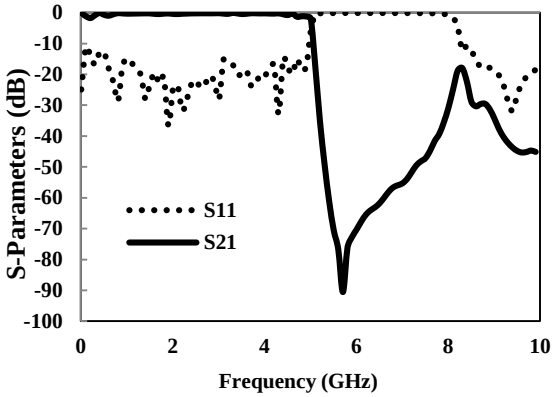

Fig. 10. The simulated S-parameters of the proposed plasmonic filter.

Moreover, we compare the scattering parameters by changing the dielectric constant of substrate material (from 2.2 to 10) as shown in Fig. 11. It can be noticed that increasing the dielectric constant results in lowering the cutoff frequency. Especially, it is pointed that with dielectric constant of 10, the cutoff frequency is reduced to 2.61GHz and a clear stop band is obtained from 2.61 to 4.11GHz with higher rejection level up to -116 dB at 3.31GHz.

Additionally, we observe the magnitude distribution of electric field by numerical simulations on a xy plane 1mm above the structure as shown in Fig. 12, at an in-band (top) and out of band (bottom) frequency of 2.5 and 5.6 GHz, respectively. It can be noticed that at the in-band frequency, the surface waves transmit effectively from one end to the far end of the filter with an underlying lossless substrate material. Evidently, the SSPPs confine more strongly inside the semi-circular grooves.

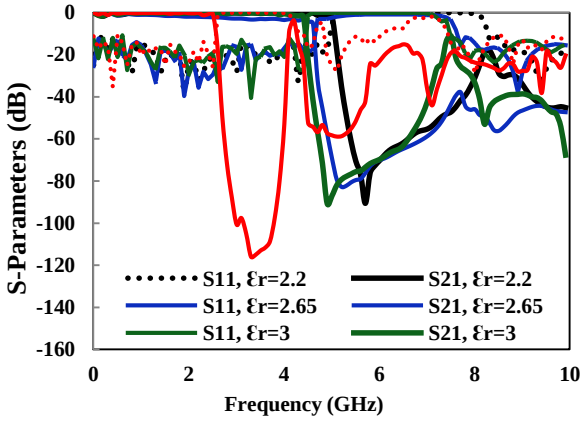

Fig. 11. The effect of varying dielectric constant on S-parameters of the proposed plasmonic filter.

It can be observed that the magnitude of electric field at both ends is approximately the same, demonstrating a negligible transmission loss in the passband. On the other hand, at out-band frequency of 5.6 GHz, the SSPPs unambiguously stop propagating right from the beginning of the Region C, therefore confirming the envisaged response in the stopband region. Figure 13 presents the magnitude distribution of magnetic field at an in-band frequency of 2.5 GHz and demonstrates that H-field profoundly confines in the depth of the groove.

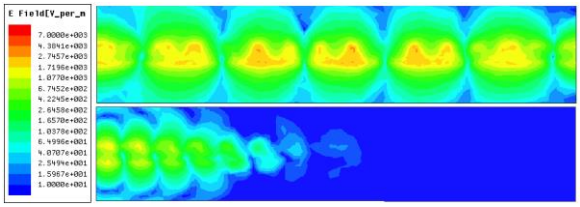

Fig. 12. The simulated magnitude electric field distribution showing confinement and propagation at (top) 2.5 GHz (bottom) 5.6 GHz.

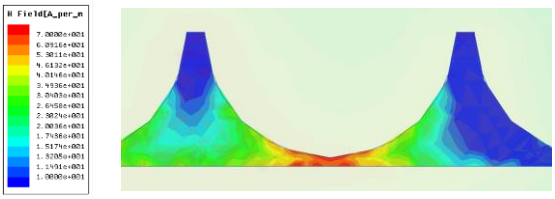

Fig. 13. The simulated magnitude magnetic field, showing the confinement inside the grooves at 2.5 GHz (A portion of SSPPs filter).

Table 1: Comparison of the proposed plasmonic filter with earlier works

Ref.	f_c (GHz)	Return Loss (dB)	Upper band Rejection Range	Filter Type	Length L	Compare L	Width W	Compare W
This Work	4.91	< -12.5	5.1 GHz	Low-Pass	230	---	45	---
[22]	12.4	< -7.5	7.6 GHz	Low-Pass	412	79%	65.2	45%
[20]	11.4	< -11	18.6 GHz	Low-Pass	200	-13%	50	12%
[25]	7.9	< -12	2.1 GHz	Low-Pass	130	-43%	20	-55%
[29]	13	< -10	2 GHz	NA	97	-57%	50	12%
[30]	12.3	< -9	1.7 GHz	Low-Pass	320	40%	70.8	58%

A comparison of the proposed plasmonic filter with previously published researches is presented in Table 1. Although the dimensions of the structure are slightly larger than some of the listed filters, comparatively, it comes up with the lowest cutoff frequency which has not been reported yet. Besides, it has good return loss in the passband with a superior stopband frequency range. Keeping in view all above demonstrations, it is proposed that such kind of SSPPs structure can find prospective use in numerous plasmonic circuits and systems.

IV. CONCLUSION

In this work, we investigate the dispersion relations of spoof SPPs for planar metallic structures having different shaped geometries. It is shown that the surface textures and groove shapes play a substantial role in defining the confinement of SSPPs in subwavelength frequency regime. Firstly, the comparison is illustrated for normalized DCs by varying depth of circular grooves structure. Afterward, DCs relations are assessed among rectangular, circular and Vee-grooves engineered on the metallic strip by varying width, and period of the structure. It has been clearly found that dispersion characteristics can be determined and asymptotic frequency can be tuned by engineering the surface's geometric parameters at will. Although the rectangular grooves performance is explicitly preeminent, the circular groove efficiency is comparable to rectangular groove structure, while it is much superior to Vee-groove structure and MS line. Likewise, the confinement of these surface waves is dependent on the period length of the structure as well as on the corrugation width and depth. A low-pass plasmonic filter has been designed based on the semi-circular grooves on planar metallic strip with two conversion sections at both ends to match the impedance and momentum of MS and the plasmonic waveguide. S-parameters and magnitude E-field distribution results show excellent transmission performance from MS to a plasmonic waveguide. The confinement of such SSPPs depends on the geometric parameters that may be useful to fine-tune the cutoff frequencies and in developing advanced plasmonic filters to be applied in integrated circuits at the microwave frequency.

ACKNOWLEDGMENT

This work was supported in part by the National Natural Science Foundation of China (Grant No. 61774014) and the Fundamental Research Funds for the Central Universities (Grant No. FRF-BD-18-016A).

REFERENCES

[1] T. W. Ebbesen, H. J. Lezec, H. Ghaemi, T. Thio, and P. Wolff, "Extraordinary optical transmission through sub-wavelength hole arrays," *Nature*, vol. 391, no. 6668, p. 667, 1998.

[2] X. Qian, X. Peng, D. Anasari. Q. Yin-Goen, G. Chen, D. Shin, L. Yang, A. Young, M. Wang, and S. Nie, "In vivo tumor targeting and spectroscopic detection with surface-enhanced Raman nano-particle tags," *Nature Biotechnology*, vol. 26, no. 1, p. 83, 2008.

[3] J. Homola, S. S. Yee, and G. Gauglitz, "Surface plasmon resonance sensors," *Sensors and Actuators B: Chemical*, vol. 54, no. 1, pp. 3-15, 1999.

[4] K. A. Willets and R. P. Van Duyne, "Localized surface plasmon resonance spectroscopy and sensing," *Annu. Rev. Phys. Chem*., vol. 58, pp. 267-297, 2007.

[5] E. Ozbay, "Plasmonics: Merging photonics and electronics at nanoscale dimensions," *Science*, vol. 311, no. 5758, pp. 189-193, 2006.

[6] L. Feng, K. A. Tetz, B. Slutsky, V. Lomakin, and Y. Fainman, "Fourier plasmonics: Diffractive focusing of in-plane surface plasmon polariton waves," *Applied Physics Letters*, vol. 91, no. 8, p. 081101, 2007.

[7] J. R. Lakowicz, "Plasmonics in biology and plasmon-controlled fluorescence," *Plasmonics*, vol. 1, no. 1, pp. 5-33, 2006.

[8] W. L. Barnes, W. A. Murray, J. Dintinger, E. Devaux, and T. Ebbesen, "Surface plasmon polaritons and their role in the enhanced trans-mission of light through periodic arrays of sub-wavelength holes in a metal film," *Physical Review Letters*, vol. 92, no. 10, p. 107401, 2004.

[9] J. F. O'Hara, R. D. Averitt, and A. J. Taylor, "Prism coupling to terahertz surface plasmon polaritons," *Optics Express*, vol. 13, no. 16, pp. 6117-6126,

2005.

[10] H. Raether, "Surface plasmons on smooth surfaces," in *Surface Plasmons on Smooth and Rough Surfaces and on Gratings*: *Springer*, pp. 4-39, 1988.

[11] J. Pendry, L. Martin-Moreno, and F. Garcia-Vidal, "Mimicking surface plasmons with structured surfaces," *Science*, vol. 305, no. 5685, pp. 847-848, 2004.

[12] A. P. Hibbins, B. R. Evans, and J. R. Sambles, "Experimental verification of designer surface plasmons," *Science*, vol. 308, no. 5722, pp. 670-672, 2005.

[13] L. Martin-Moreno and F. Garcia-Vidal, "Optical transmission through circular hole arrays in optically thick metal films," *Optics Express*, vol. 12, no. 16, pp. 3619-3628, 2004.

[14] F. J. Garcia-Vidal, L. Martin-Moreno, T. Ebbesen, and L. Kuipers, "Light passing through subwavelength apertures," *Reviews of Modern Physics*, vol. 82, no. 1, p. 729, 2010.

[15] X. Shou, A. Agrawal, and A. Nahata, "Role of metal film thickness on the enhanced transmission properties of a periodic array of subwavelength apertures," *Optics Express*, vol. 13, no. 24, pp. 9834-9840, 2005.

[16] X. Wan and T. J. Cui, "Guiding spoof surface plasmon polaritons by infinitely thin grooved metal strip," *Aip Advances*, vol. 4, no. 4, p. 047137, 2014.

[17] X. Gao, L. Zhou, Z. Liao, H. F. Ma, and T. J. Cui, "An ultra-wideband surface plasmonic filter in microwave frequency," *Applied Physics Letters*, vol. 104, no. 19, p. 191603, 2014.

[18] T. Søndergaard and S. I. Bozhevolnyi, "Surface-plasmon polariton resonances in triangular-groove metal gratings," *Physical Review B*, vol. 80, no. 19, p. 195407, 2009.

[19] C. Chen, "A new kind of spoof surface plasmon polaritons structure with periodic loading of T-shape grooves," *AIP Advances*, vol. 6, no. 10, p. 105003, 2016.

[20] R. S. Anwar, Y. Wei, L. Mao, X. Li, and H. Ning, "Novel spoof surface plasmon polaritons on a planar metallic strip with periodic semi-elliptical grooves at microwave frequency," *Journal of Electromagnetic Waves and Applications*, pp. 1-13, 2018.

[21] R. S. Anwar, H. Ning, L. Mao, and "Recent advancements in surface plasmon polaritons-plasmonics in subwavelength structures at microwave and terahertz regimes," *Digital Communications and Networks*, 2017.

[22] H. C. Zhang, Q. Zhang, J. F. Liu, W. Tang, Y. Fan, and T. J. Cui, "Smaller-loss planar SPP transmission line than conventional microstrip in microwave frequencies," *Scientific Reports*, vol. 6, 2016.

[23] X. Liu, Y. Feng, B. Zhu, J. Zhao, and T. Jiang, "High-order modes of spoof surface plasmonic wave transmission on thin metal film structure," *Optics Express*, vol. 21, no. 25, pp. 31155-31165, 2013.

[24] X. Shen, T. J. Cui, D. Martin-Cano, and F. J. Garcia-Vidal, "Conformal surface plasmons propagating on ultrathin and flexible films," *Proceedings of the National Academy of Sciences*, vol. 110, no. 1, pp. 40-45, 2013.

[25] J. Xu, Z. Li, L. Liu. C. Chen, B. Xu, P. Ning, and C. Gu., "Low-pass plasmonic filter and its miniaturization based on spoof surface plasmon polaritons," *Optics Communications*, vol. 372, pp. 155-159, 2016.

[26] J. Wang, H. Ning, Q. Xiong, and L. Mao, "A compact narrow-band bandstop filter using spiral-shaped defected microstrip structure," *Radio-engineering*, vol. 23, no. 1, 2014.

[27] H. Ning, J. Wang, Q. Xiong, and L. Mao, "Design of planar dual and triple narrow-band bandstop filters with independently controlled stopbands and improved spurious response," *Progress In Electromagnetics Research*, vol. 131, pp. 259-274, 2012.

[28] H. Ning, J. Wang, Q. Xiong, H. Liu, and L. Mao, "A compact quad-band bandstop filter using dual-plane defected structures and open-loop resonators," *IEICE Electronics Express*, vol. 9, no. 21, pp. 1630-1636, 2012.

[29] S. Zhou, *et al.*, "Spoof surface plasmon polaritons power Divider with large Isolation," *Scientific Reports*, vol. 8, no. 1, p. 5947, 2018.

[30] H. F. Ma, X. Shen, Q. Cheng, W. X. Jiang, and T. J. Cui, "Broadband and high-efficiency conversion from guided waves to spoof surface plasmon polaritons," *Laser & Photonics Reviews*, vol. 8, no. 1, pp. 146-151, 2014.